

Modeling of Wave Propagation in General Dispersive Materials with Efficient ADE-WLP-FDTD Method

Jun Quan¹ and Wei-Jun Chen^{2, *}

Abstract—Within the framework of the finite-difference time-domain (FDTD) and the weighted Laguerre polynomials (WLPs), we derive an effective update equation of the electromagnetic in the dispersive media by introducing the factorization-splitting (FS) schemes and auxiliary differential equation (ADE). As two examples, we employ a 2-D parallel plate waveguide loaded with two dispersive medium columns and a thin graphene sheet to calculate the plane wave propagation by using the FS-ADE-WLP-FDTD method. Compared with the ADE-FDTD and the ADE-WLP-FDTD methods, the results from our proposed method show its accuracy and efficiency for dispersive media simulation.

1. INTRODUCTION

The finite-difference time-domain (FDTD) method has been widely used for electromagnetic modeling due to its easy implementation [1]. However, because of Courant-Friedrich-Levy (CFL) stability constraint, the conventional FDTD is not very suitable for electromagnetic problems which involve fine grid division. To eliminate the limitation, some techniques, e.g., alternating-direction implicit (ADI) [2–4] and locally one-dimensional (LOD) [5–7] methods, were proposed. Although these techniques can get more accurate simulation results and higher computational efficiency than the conventional FDTD, a large time step inevitably results in a large numerical dispersion error. Also, an unconditionally stable FDTD method using Laguerre polynomials has been proposed [8]. This marching-on-in-order scheme shows better efficiency than the conventional FDTD method when analyzing multi-scale structure.

Based on auxiliary differential equation (ADE), an unconditionally stable WLP-FDTD was proposed to simulate electromagnetic wave propagation in general dispersive materials [9]. The method introduces an ADE technique which establishes the relationship between the electric displacement vector and electric field intensity with a differential equation rather than a convolution integral. However, it leads to a huge sparse matrix equation, which is very challenging to solve. To solve the huge sparse matrix equation, an efficient algorithm is regularly used to implement the WLP-FDTD method [10], in which the huge sparse matrix equation is solved into a sub-steps procedure with a factorized-splitting scheme.

In this paper, a hybrid algorithm, known as factorization-splitting ADE-WLP-FDTD, is presented to improve its simulation performance. Based on the FS and ADE technique, our proposed algorithm only solves two tri-diagonal matrices and computes one explicit equation in 2-D problem. In comparison with the conventional implementation, less CPU runtime is spent. The accuracy and efficiency of the proposed method is verified by simulating electromagnetic wave propagation in a variety of dispersive media.

Received 19 November 2015, Accepted 11 January 2016, Scheduled 27 January 2016

* Corresponding author: Wei-Jun Chen (chenw-j@163.com).

¹ School of Physics Science and Technology, Lingnan Normal University, Zhanjiang 524048, China. ² School of Information Science and Technology, Lingnan Normal University, Zhanjiang 524048, China.

2. MATHEMATICAL FORMULATION

With lossless and dispersive media, the Maxwell's equations read

$$\frac{\partial \mathbf{D}(\mathbf{r}, t)}{\partial t} = \nabla \times \mathbf{H}(\mathbf{r}, t) - \mathbf{J}(\mathbf{r}, t) \quad (1)$$

$$\frac{\partial \mathbf{H}(\mathbf{r}, t)}{\partial t} = -\frac{1}{\mu_0} \nabla \times \mathbf{E}(\mathbf{r}, t) \quad (2)$$

where μ_0 is the magnetic permeability of free space. The electric displacement vector \mathbf{D} is related to the electric field intensity \mathbf{E} through the relative dielectric constant ε_r of the local tissue by

$$\mathbf{D}(\omega) = \varepsilon_0 \varepsilon_r(\omega) \mathbf{E}(\omega) \quad (3)$$

where ε_0 is the electric permittivity in free space. In the frequency domain, ε_r can be written as [9, 11]

$$\varepsilon_r(\omega) = \varepsilon_\infty \left(1 + \sum_n^{N_d} \frac{a_n}{b_n + j\omega c_n - d_n \omega^2} \right) \quad (4)$$

where ε_∞ is the infinite dielectric constant, ω the angular frequency, and a_n , b_n , c_n and d_n are known constants determined by the properties of the electric fields $\mathbf{E}(\omega)$. Substituting Eq. (4) into Eq. (3), we get

$$\mathbf{D}(\omega) = \varepsilon_0 \varepsilon_\infty \left[\mathbf{E}(\omega) + \sum_n^{N_d} \mathbf{S}_n(\omega) \right] \quad (5)$$

with

$$\mathbf{S}_n(\omega) = \frac{a_n}{b_n + j\omega c_n - d_n \omega^2} \mathbf{E}(\omega) \quad (6)$$

In terms of the transition relationship $j\omega \rightarrow \partial/\partial t$, Eqs. (5) and (6) can be casted into

$$\mathbf{D}(\mathbf{r}, t) = \varepsilon_0 \varepsilon_\infty \left(\mathbf{E}(\mathbf{r}, t) + \sum_{n=1}^{N_d} \mathbf{S}_n(\mathbf{r}, t) \right) \quad (7)$$

$$b_n \mathbf{S}_n(\mathbf{r}, t) + c_n \frac{\partial \mathbf{S}_n(\mathbf{r}, t)}{\partial t} + d_n \frac{\partial^2 \mathbf{S}_n(\mathbf{r}, t)}{\partial t^2} = a_n \mathbf{E}(\mathbf{r}, t) \quad (8)$$

Substituting Eq. (7) into Eq. (1) results in

$$\frac{\partial \mathbf{E}(\mathbf{r}, t)}{\partial t} + \sum_{n=1}^{N_d} \frac{\partial \mathbf{S}_n(\mathbf{r}, t)}{\partial t} = \frac{1}{\varepsilon_0 \varepsilon_\infty} \nabla \times \mathbf{H}(\mathbf{r}, t) - \frac{1}{\varepsilon_0 \varepsilon_\infty} \mathbf{J}(\mathbf{r}, t) \quad (9)$$

Using the weighted Laguerre basis functions $\varphi_q(st)$, the field components can be expanded as [8]

$$\{\mathbf{E}, \mathbf{H}, \mathbf{S}(\mathbf{r}, t)\} = \sum_{q=0}^{\infty} \{\mathbf{E}^q, \mathbf{H}^q, \mathbf{S}^q(\mathbf{r})\} \varphi_q(st) \quad (10)$$

where s , q are time-scale factor and the order of Laguerre functions, respectively. For an arbitrary field component $\mathbf{U}(\mathbf{r}, t)$, for example, \mathbf{E} , \mathbf{H} , $\mathbf{S}(\mathbf{r}, t)$, etc., the first and second derivatives of $\mathbf{U}(\mathbf{r}, t)$ obey the following equations [8, 12], respectively,

$$\frac{\partial \mathbf{U}(\mathbf{r}, t)}{\partial t} = s \sum_{q=0}^{\infty} \left[0.5 \mathbf{U}^q(\mathbf{r}) + \sum_{k=0, q>0}^{q-1} \mathbf{U}^k(\mathbf{r}) \right] \varphi_q(st) \quad (11)$$

$$\frac{\partial^2 \mathbf{U}(\mathbf{r}, t)}{\partial t^2} = s^2 \sum_{q=0}^{\infty} \left[\frac{\mathbf{U}^q(\mathbf{r})}{4} + \sum_{k=0, q>0}^{q-1} (q-k) \mathbf{U}^k(\mathbf{r}) \right] \varphi_q(st) \quad (12)$$

Inserting Eqs. (10)–(12) into Eqs. (2), (8) and (9), multiplying both sides by $\varphi_p(st)$, and integrating over $st \in [0, \infty)$, we have

$$\mathbf{E}^q(\mathbf{r}) + \sum_{n=1}^{N_d} \mathbf{S}_n^q(\mathbf{r}) = \frac{2}{s\varepsilon_0\varepsilon_\infty} \nabla \times \mathbf{H}^q(\mathbf{r}) - \frac{2}{s\varepsilon_0\varepsilon_\infty} \mathbf{J}^q(\mathbf{r}) - 2 \sum_{k=0, q>0}^{q-1} \mathbf{E}^k(\mathbf{r}) - 2 \sum_{n=1}^{N_d} \sum_{k=0, q>0}^{q-1} \mathbf{S}_n^k(\mathbf{r}) \quad (13)$$

$$\mathbf{S}_n^q(\mathbf{r}) = \frac{1}{A_n} \left\{ a_n \mathbf{E}^q(\mathbf{r}) - \sum_{k=0, q>0}^{q-1} [c_n s + d_n s^2 (q-k)] \mathbf{S}_n^k(\mathbf{r}) \right\} \quad (14)$$

$$\mathbf{H}^q(\mathbf{r}) = -\frac{2}{s\mu_0} \nabla \times \mathbf{E}^q(\mathbf{r}) - 2 \sum_{k=0, q>0}^{q-1} \mathbf{H}^k(\mathbf{r}) \quad (15)$$

where $\mathbf{J}^q(\mathbf{r}) = \int_0^{T_f} \mathbf{J}(\mathbf{r}, t) \varphi_p(st) d(st)$, $A_n = b_n + 0.5sc_n + 0.25s^2d_n$, and T_f is a finite time interval. Substituting Eq. (14) into Eq. (13), we may then write, instead of Eq. (13),

$$\begin{aligned} \left(1 + \sum_{n=1}^{N_d} \frac{a_n}{A_n} \right) \mathbf{E}^q(\mathbf{r}) &= -2 \sum_{k=0, q>0}^{q-1} \mathbf{E}^k(\mathbf{r}) + \sum_{n=1}^{N_d} \left(\frac{sa_n}{A_n} - 2 \right) \sum_{k=0, q>0}^{q-1} \mathbf{S}_n^k(\mathbf{r}) \\ &+ \frac{2}{s\varepsilon_0\varepsilon_\infty} \nabla \times \mathbf{H}^q(\mathbf{r}) - \frac{2}{s\varepsilon_0\varepsilon_\infty} \mathbf{J}^q(\mathbf{r}) + \frac{s^2d}{A_n} \sum_{n=1}^{N_d} \sum_{k=0, q>0}^{q-1} (q-k) \mathbf{S}_n^k(\mathbf{r}) \end{aligned} \quad (16)$$

Hence, Eqs. (15) and (16) can be written as a matrix equation form [8]. After obtaining the auxiliary differential variable \mathbf{S} from Eq. (14), the electric fields are obtained by solving the matrix equation.

For the sake of simplicity, in the following sections we will employ a 2-D TE_z case and single pole dispersive media ($N_d = 1$) to describe the procedures for deriving the FS-ADE-WLP-FDTD algorithm, then the z -component of $\mathbf{H}^q(\mathbf{r})$ in (15) reads

$$H_z^q(\mathbf{r}) = \sum_{\substack{\alpha, \beta \\ \alpha \neq \beta}} \sigma b D_\alpha E_\beta^q(\mathbf{r}) + V_H^{q-1}(\mathbf{r}) \quad (17)$$

where $b = 2/(\mu_0 s)$, $V_H^{q-1}(\mathbf{r}) = -2 \sum_{k=0, q>0}^{q-1} H_z^k(\mathbf{r})$. $D_\alpha = \partial/\partial\alpha$ ($\alpha, \beta = x, y$), is the first-order partial differential operator, and $\alpha = x$, $\sigma = -1$, $\alpha = y$, $\sigma = 1$. The α -components of $\mathbf{E}^q(\mathbf{r})$ and $\mathbf{S}_1^q(\mathbf{r})$ in Eqs. (14) and (16) are given by

$$E_\alpha^q(\mathbf{r}) = A_\alpha D_\beta H_z^q(\mathbf{r}) + J_{E\alpha}^q(\mathbf{r}) + V_{E\alpha}^{q-1}(\mathbf{r}) + V_{S\alpha}^{q-1}(\mathbf{r}) \quad (18)$$

$$S_{1\alpha}^q(\mathbf{r}) = 1/A_{1\alpha} \left\{ a_{1\alpha} E_\alpha^q(\mathbf{r}) - \sum_{k=0, q>0}^{q-1} [c_{1\alpha} s + d_{1\alpha} s^2 (q-k)] S_{1\alpha}^k(\mathbf{r}) \right\} \quad (19)$$

where A_α , $J_{E\alpha}^q$, $V_{E\alpha}^{q-1}$ and $V_{S\alpha}^{q-1}$ are given by

$$A_\alpha = A_{1\alpha} / [0.5\varepsilon_0\varepsilon_{\alpha, \infty} s (a_{1\alpha} + A_{1\alpha})] \quad (20)$$

$$J_{E\alpha}^q = -A_{1\alpha} J_\alpha^q(\mathbf{r}) / [0.5\varepsilon_0\varepsilon_{\alpha, \infty} s (a_{1\alpha} + A_{1\alpha})] \quad (21)$$

with J_α^q describing the incident electric current excitation source along α axes.

$$V_{E\alpha}^{q-1}(\mathbf{r}) = -2A_{1\alpha} / (a_{1\alpha} + A_{1\alpha}) \sum_{k=0, q>0}^{q-1} E_\alpha^k(\mathbf{r}) \quad (22)$$

$$V_{S\alpha}^{q-1}(\mathbf{r}) = (c_{1\alpha} s - 2A_{1\alpha}) / (a_{1\alpha} + A_{1\alpha}) \sum_{k=0, q>0}^{q-1} S_{1\alpha}^k(\mathbf{r}) + d_{1\alpha} s^2 / (a_{1\alpha} + A_{1\alpha}) \sum_{k=0, q>0}^{q-1} (q-k) S_{1\alpha}^k(\mathbf{r}) \quad (23)$$

Similar to the derivational procedure in [10], Eqs. (17)–(19) can be written as a matrix form

$$\mathbf{W}_E^q = \mathbf{D}_H \mathbf{W}_H^q + \mathbf{J}_E^q + \mathbf{V}_E^{q-1} + \mathbf{V}_S^{q-1} \quad (24)$$

$$\mathbf{W}_H^q = \mathbf{D}_E \mathbf{W}_E^q + \mathbf{V}_H^{q-1} \quad (25)$$

where $\mathbf{W}_E^q = [E_x^q \ E_y^q]^T$, $\mathbf{W}_H^q = [H_z^q]$, $\mathbf{J}_E^q = [J_{E_x}^q \ J_{E_y}^q]^T$, $\mathbf{D}_H = [A_x D_y - A_y D_x]^T$, $\mathbf{D}_E = [b D_y - b D_x]$, $\mathbf{V}_E^{q-1} = [V_{E_x}^{q-1} \ V_{E_y}^{q-1}]^T$, $\mathbf{V}_S^{q-1} = [V_{S_x}^{q-1} \ V_{S_y}^{q-1}]^T$. Combining Eqs. (24) and (25) leads to

$$\begin{bmatrix} \mathbf{W}_E^q \\ \mathbf{W}_H^q \end{bmatrix} = \begin{bmatrix} 0 & \mathbf{D}_H \\ \mathbf{D}_E & 0 \end{bmatrix} \begin{bmatrix} \mathbf{W}_E^q \\ \mathbf{W}_H^q \end{bmatrix} + \begin{bmatrix} \mathbf{J}_E^q \\ 0 \end{bmatrix} + \begin{bmatrix} \mathbf{V}_E^{q-1} \\ \mathbf{V}_H^{q-1} \end{bmatrix} + \begin{bmatrix} \mathbf{V}_S^{q-1} \\ 0 \end{bmatrix} \quad (26)$$

Let $\mathbf{W}_{EH}^q = [\mathbf{W}_E^q \ \mathbf{W}_H^q]^T$, $\mathbf{J}_{EH}^q = [\mathbf{J}_E^q \ 0]$, $\mathbf{V}_{EH}^{q-1} = [\mathbf{V}_E^{q-1} \ \mathbf{V}_H^{q-1}]$ and $\mathbf{V}_{SH}^{q-1} = [\mathbf{V}_S^{q-1} \ 0]^T$, then Eq. (26) becomes

$$(\mathbf{I} - \mathbf{A} - \mathbf{B}) \mathbf{W}_{EH}^q = \mathbf{V}_{EH}^{q-1} + \mathbf{V}_{SH}^{q-1} + \mathbf{J}_{EH}^q \quad (27)$$

with

$$\mathbf{A} = \begin{bmatrix} 0 & \mathbf{D}_{Ha} \\ \mathbf{D}_{Ea} & 0 \end{bmatrix} = \begin{bmatrix} 0 & 0 & 0 \\ 0 & 0 & -A_y D_x \\ 0 & -b D_x & 0 \end{bmatrix}$$

$$\mathbf{B} = \begin{bmatrix} 0 & \mathbf{D}_{Hb} \\ \mathbf{D}_{Eb} & 0 \end{bmatrix} = \begin{bmatrix} 0 & 0 & A_x D_y \\ 0 & 0 & 0 \\ b D_y & 0 & 0 \end{bmatrix}$$

Adding a perturbation term $\mathbf{AB}(\mathbf{W}_{EH}^q - \mathbf{V}_{EH}^{q-1})$ to Eq. (27), we can obtain the factorized form

$$(\mathbf{I} - \mathbf{A})(\mathbf{I} - \mathbf{B}) \mathbf{W}_{EH}^q = \mathbf{ABV}_{EH}^{q-1} + \mathbf{V}_{EH}^{q-1} + \mathbf{V}_{SH}^{q-1} + \mathbf{J}_{EH}^q \quad (28)$$

Equation (28) can be computed into two sub-steps as following,

$$(\mathbf{I} - \mathbf{A}) \mathbf{W}_{EH}^{*q} = (\mathbf{I} + \mathbf{B}) \mathbf{V}_{EH}^{q-1} + \mathbf{V}_{SH}^{q-1} + \mathbf{J}_{EH}^q \quad (29)$$

$$(\mathbf{I} - \mathbf{B}) \mathbf{W}_{EH}^q = \mathbf{W}_{EH}^{*q} - \mathbf{BV}_{EH}^{q-1} \quad (30)$$

where $\mathbf{W}_{EH}^{*q} = [\mathbf{W}_E^{*q} \ \mathbf{W}_H^{*q}]^T = [\mathbf{E}_x^{*q} \ \mathbf{E}_y^{*q} \ \mathbf{H}_z^{*q}]^T$. Using Eqs. (29) and (30) to solve Eq. (28) with some manipulations, we get

$$(\mathbf{I} - \mathbf{D}_{Ha} \mathbf{D}_{Ea}) \mathbf{W}_E^{*q} = (\mathbf{D}_{Ha} + \mathbf{D}_{Hb}) \mathbf{V}_H^{q-1} + (\mathbf{I} + \mathbf{D}_{Ha} \mathbf{D}_{Eb}) \mathbf{V}_E^{q-1} + \mathbf{V}_S^{q-1} + \mathbf{J}_E^q \quad (31)$$

$$(\mathbf{I} - \mathbf{D}_{Hb} \mathbf{D}_{Eb}) \mathbf{W}_E^q = (\mathbf{I} + \mathbf{D}_{Hb} \mathbf{D}_{Ea}) \mathbf{W}_E^{*q} \quad (32)$$

$$\mathbf{W}_H^q = \mathbf{D}_{Eb} \mathbf{W}_E^q + \mathbf{D}_{Ea} \mathbf{W}_E^{*q} + \mathbf{V}_H^{q-1} \quad (33)$$

Expanding Eqs. (31)–(33) leads to

$$E_x^{*q} = A_x D_y V_H^{q-1} + V_{E_x}^{q-1} + V_{S_x}^{q-1} + J_{E_x}^q \quad (34)$$

$$E_y^q = E_y^{*q} \quad (35)$$

$$(I - b A_y D_{2x}) E_y^{*q} = -A_y D_x V_H^{q-1} + V_{E_y}^{q-1} - b A_y D_x D_y V_{E_x}^{q-1} + V_{S_y}^{q-1} + J_{E_y}^q \quad (36)$$

$$(I - b A_x D_{2y}) E_x^q = E_x^{*q} - b A_x D_y D_x E_y^{*q} \quad (37)$$

$$H_z^q = b D_y E_x^q - b D_x E_y^{*q} + V_H^{q-1} \quad (38)$$

where $D_{2\alpha}$ ($\alpha = x, y$) is the second-order partial differential operator. Substituting Eqs. (34) and (35) into Eqs. (36)–(38), we have

$$(I - b A_y D_{2x}) E_y^q = -A_y D_x V_H^{q-1} + V_{E_y}^{q-1} - b A_y D_x D_y V_{E_x}^{q-1} + V_{S_y}^{q-1} + J_{E_y}^q \quad (39)$$

$$(I - b A_x D_{2y}) E_x^q = A_x D_y V_H^{q-1} + V_{E_x}^{q-1} + V_{S_x}^{q-1} + J_{E_x}^q - b A_x D_y D_x E_y^q \quad (40)$$

$$H_z^q = b D_y E_x^q - b D_x E_y^q + V_H^{q-1} \quad (41)$$

Equations (39)–(41) are the update equations for efficient 2-D ADE-WLP-FDTD method. According to the central-difference scheme introduced by Yee, we discretize space Equations (39)–(41) and obtain

the following form:

$$\begin{aligned} & \left[1 + \frac{bA_y |_{i,j}}{\Delta \bar{x} |_{i,j}} \left(\frac{1}{\Delta x |_{i,j}} + \frac{1}{\Delta x |_{i-1,j}} \right) \right] E_y^q |_{i,j} - \frac{bA_y |_{i+1,j}}{\Delta x |_{i,j} \Delta \bar{x} |_{i,j}} E_y^q |_{i+1,j} - \frac{bA_y |_{i-1,j}}{\Delta x |_{i-1,j} \Delta \bar{x} |_{i,j}} E_y^q |_{i-1,j} \\ &= \frac{A_y |_{i,j}}{\Delta \bar{x} |_{i,j}} \left(V_H^{q-1} |_{i,j} - V_H^{q-1} |_{i-1,j} \right) + J_{E_y}^q |_{i,j} + V_{E_y}^{q-1} |_{i,j} + V_{S_y}^{q-1} |_{i,j} \\ & \quad - \frac{A_y |_{i,j} b}{\Delta y |_{i,j} \Delta \bar{x} |_{i,j}} \left(V_{E_x}^{q-1} |_{i,j+1} - V_{E_x}^{q-1} |_{i,j} - V_{E_x}^{q-1} |_{i-1,j+1} + V_{E_x}^{q-1} |_{i-1,j} \right) \end{aligned} \quad (42)$$

$$\begin{aligned} & \left[1 + \frac{bA_x |_{i,j}}{\Delta \bar{y} |_{i,j}} \left(\frac{1}{\Delta y |_{i,j-1}} + \frac{1}{\Delta y |_{i,j}} \right) \right] E_x^q |_{i,j} - \frac{bA_x |_{i,j+1}}{\Delta y |_{i,j} \Delta \bar{y} |_{i,j}} E_x^q |_{i,j+1} - \frac{bA_x |_{i,j-1}}{\Delta y |_{i,j-1} \Delta \bar{y} |_{i,j}} E_x^q |_{i,j-1} \\ &= -\frac{A_x |_{i,j}}{\Delta \bar{y} |_{i,j}} \left(V_H^k |_{i,j} - V_H^k |_{i,j-1} \right) + V_{E_x}^{q-1} |_{i,j} + J_{E_x}^q |_{i,j} + V_{S_x}^k |_{i,j} \\ & \quad - \frac{A_x |_{i,j} b}{\Delta x |_{i,j} \Delta \bar{y} |_{i,j}} \left(E_y^q |_{i+1,j} - E_y^q |_{i,j} - E_y^q |_{i+1,j-1} + E_y^q |_{i,j-1} \right) \end{aligned} \quad (43)$$

$$H_z^q |_{i,j} = \frac{b}{\Delta y |_{i,j}} \left(E_x^q |_{i,j+1} - E_x^q |_{i,j} \right) - \frac{b}{\Delta x |_{i,j}} \left(E_y^q |_{i+1,j} - E_y^q |_{i,j} \right) - 2 \sum_{k=0, q>0}^{q-1} H_z^k |_{i,j} \quad (44)$$

Comparing Eqs. (39) and (40) with [10], one can find that some parameters determined by dispersive media, A_α , $\alpha = x, y$ for example, are included.

3. NUMERICAL RESULTS

In order to validate the effectiveness of the FS-ADE-WLP-FDTD method, as the first example, we employ the wave transmission in a 2-D parallel plate waveguide with two dispersive medium columns, as depicted in Fig. 1. The staircase approximation is introduced to model dispersive medium columns. To improve the simulation precision, a fine grid division with cell size of $0.3 \text{ mm} \times 0.3 \text{ mm}$ is applied to the staircase region. The graded mesh is applied to rest computational regions, and the maximal cell is $10 \text{ mm} \times 10 \text{ mm}$ [9]. For simplicity, Mur's 1st-order absorbing boundary conditions are used to truncate the computational area [8].

The first dispersive medium column is Debye model, in which the relative complex permittivity is given by

$$\varepsilon_r(\omega) = \varepsilon_\infty + \frac{\varepsilon_s - \varepsilon_\infty}{1 + j\omega\tau} \quad (45)$$

where $\varepsilon_s = 4.301$, $\varepsilon_\infty = 4.096$ and $\tau = 2.294 \times 10^{-9}$. The second dispersive medium column is Lorentz model, in which the relative complex permittivity is given by

$$\varepsilon_r(\omega) = \varepsilon_\infty + (\varepsilon_s - \varepsilon_\infty) \frac{G_1 \omega_1^2}{\omega_1^2 + 2j\delta_1 \omega - \omega^2} \quad (46)$$

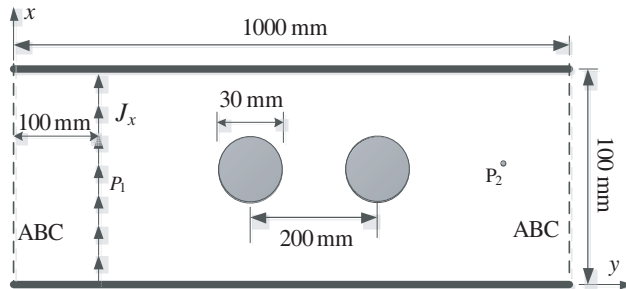


Figure 1. 2-D parallel plate waveguide with two dispersive media columns.

where $\varepsilon_s = 3$, $\varepsilon_\infty = 1.5$, $\omega_1 = 2 \times 10^9$ rad/s, $G_1 = 0.4$ and $\delta_1 = 0.1\omega_1$. A sinusoidally modulated Gaussian pulse is used as a x -incident electric current profile

$$J_x(t) = \exp \left[- \left(\frac{t - T_c}{T_d} \right)^2 \right] \sin 2\pi f_c(t - T_c) \quad (47)$$

where $T_d = 1/(2f_c)$, $T_c = 3T_d$ and $f_c = 1$ GHz. And we choose the time duration $T_f = 11.71$ ns, time scaling factor $s = 1.1902 \times 10^{10}$ and order-marching step number $N_L = 142$.

Figure 2 shows the calculated results given by the FS-ADE-WLP-FDTD, ADE-WLP-FDTD and ADE-FDTD. From their profiles, one can find that the FS-ADE-WLP-FDTD is accurate.

Table 1 shows the required computational resource and computing time for the numerical simulations. Compared with the ADE-WLP-FDTD and the ADE-FDTD, the FS-ADE-WLP-FDTD shows much improvement in computation efficiency. All calculations have been performed on an AMD Phenom II \times 6 2.80 GHz machine with 8 GB RAM.

In the second example, the transmission coefficient of wave propagation in graphene sheets is calculated, as shown in Fig. 3. Here, we also choose x -polarization as the electric current excitation, and $T_c = 3T_d$, $f_c = 5000$ GHz, the time duration $T_f = 1.5 \times 10^{-12}$ s, time scaling factor $s = 3.7699 \times 10^{14}$ and order-marching step number $N = 150$. Due to the structure with a thin layer in the computational domain, a fine grid division with the cell size of $1 \text{ nm} \times 1500 \text{ nm}$ is applied to the graphene layer. The graded mesh is applied to the rest computational regions, and the maximal cell is $1500 \text{ nm} \times 1500 \text{ nm}$. In this example, the dispersive model of grapheme can be written as

$$\varepsilon_r(\omega) = \left(1 + \frac{\sigma_0/\varepsilon_0}{j\omega - \tau\omega^2} \right) \quad (48)$$

with

$$\sigma_0 = \frac{e^2 \tau k_B T}{\pi \hbar^2 \Delta} \left(\frac{\mu_c}{k_B T} + 2 \ln \left(e^{-\frac{\mu_c}{k_B T}} + 1 \right) \right)$$

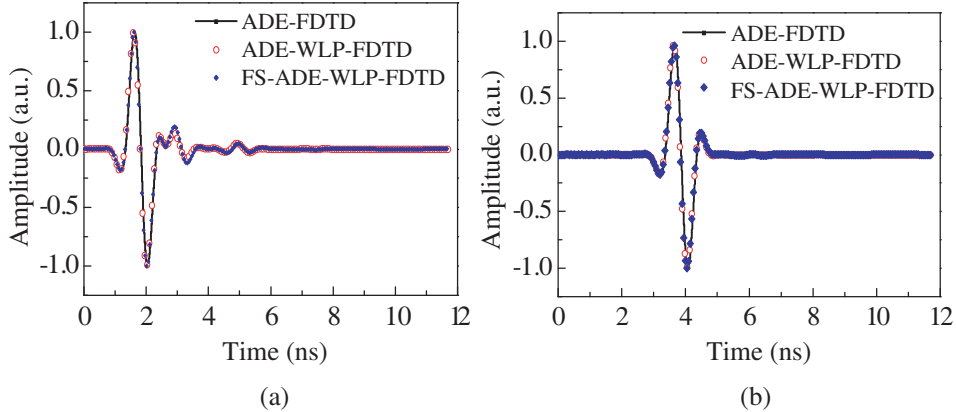


Figure 2. Transient electric fields of the x component (a) at P_1 and (b) P_2 .

Table 1. Comparison of the computational efforts for the 2-D waveguide.

Method	Δt (ps)	Meshing size	Marching-on steps	Memory (MB)	CPU time(s)
ADE-FDTD	0.5	320×120	23420	5.2	710
ADE-WLP-FDTD	30	320×120	142	103	242
FS-ADE-WLP-FDTD	30	320×120	142	97	60

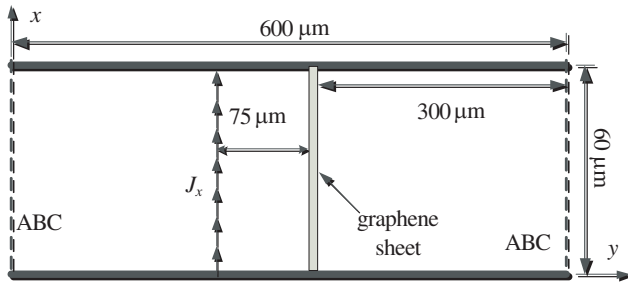


Figure 3. Diagram of computational domain for WLP-FDTD analysis of graphene sheet.

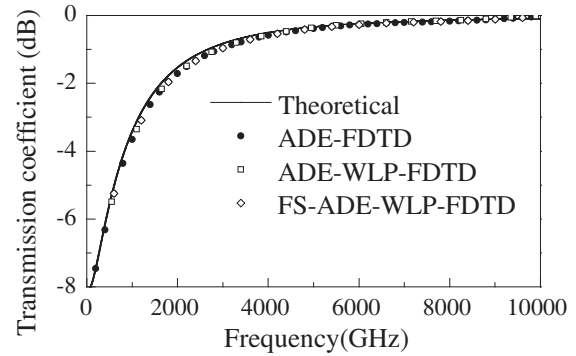


Figure 4. Transmission coefficient calculated with the FS-ADE-WLP-FDTD, ADE-FDTD, ADE-WLP-FDTD and the theoretical solution.

where Δ , e , $\hbar = h/2\pi$, k_B , T , τ and μ_c are the thickness of graphene sheets, electron charge, reduced Planck's constant, Boltzmann constant, temperature, scattering time and chemical potential, respectively [13]. Fig. 4 plots the numerical results of FS-ADE-WLP-FDTD, ADE-WLP-FDTD, ADE-FDTD and theory by setting $\Delta = 10$ nm, $\mu_c = 0.5$ eV, $T = 300$ K and $\tau = 0.5 \times 10^{-12}$ s. Compared with the theoretical solution, the accuracy of the FS-ADE-WLP-FDTD method is verified.

Table 2 shows the comparison of the computing times among the three numerical methods. In Table 2, the FS-ADE-WLP-FDTD method also shows much more improvement in computation efficiency than the ADE-WLP-FDTD and ADE-FDTD methods.

Table 2. Comparison of the computational efforts for the graphene sheet.

Method	Δt (fs)	Meshing size	Marching-on steps	Memory (MB)	CPU time(s)
ADE-FDTD	1.67×10^{-3}	462×40	9×10^5	29	1722
ADE-WLP-FDTD	2.5	462×40	150	52	52
FS-ADE-WLP-FDTD	2.5	462×40	150	50	10

4. CONCLUSION

An ADE-WLP-FDTD method based on factorization splitting technique for general dispersive media is presented in this paper. Compared with the ADE-FDTD and ADE-WLP-FDTD, the FS-ADE-WLP-FDTD method can reduce the calculation burden. Two examples verify the accuracy and efficiency of the FS-ADE-WLP-FDTD method.

ACKNOWLEDGMENT

We gratefully acknowledge the support by the National Natural Science Foundation of China (Grant No. 11304276), the Natural Science Foundation of Guangdong Province, China (Grant No. 2014A030307035), the Cultivation of Innovative Talents in Colleges and Universities of Guangdong (Grant No. LYM10098) and the Natural Science Foundation of Lingnan Normal University (Grant No. ZL1004 ZL1506).

REFERENCES

1. Taflov, A. and S. C. Hagness, *Computational Electrodynamics: The Finite-difference Time-domain Method*, 2nd Edition, Artech House, Boston, MA, 2005.
2. Namiki, T., “A new FDTD algorithm based on alternating-direction implicit method,” *IEEE Trans. Microw. Theory Tech.* Vol. 7, No. 10, 2003–2007, Oct. 1999.
3. Kantartzis, N. V., T. T. Zygiridis, and T. D. Tsiboukis, “An unconditionally stable higher order ADI-FDTD technique for the dispersionless analysis of generalized 3-D EMC structures,” *IEEE Trans. Magn.*, Vol. 40, No. 3, 1436–1439, Mar. 2004.
4. Kantartzis, N. V., D. L. Sounas, C. S. Antonopoulos, and T. D. Tsiboukis, “A wideband ADI-FDTD algorithm for the design of double negative metamaterial-based waveguides and antenna substrates,” *IEEE Trans. Magn.*, Vol. 43, No. 4, 1329–1332, Apr. 2007.
5. Shibayama, J., M. Muraki, J. Yamauchi, and H. Nakano, “Efficient implicit FDTD algorithm based on locally one-dimensional scheme,” *Electron. Lett.*, Vol. 41, No. 19, 1046–1047, Sep. 2005.
6. Rana, M. and A. Mohan, “Segmented-LOD-FDTD for electromagnetic propagation inside large complex tunnels,” *IEEE Trans. Magn.*, Vol. 48, No. 2, 223–226, Feb. 2012.
7. Kantartzis, N. V., T. Ohtani, and Y. Kanai, “Accuracy-adjustable nonstandard LOD-FDTD schemes for the design of carbon nanotube interconnects and nanocomposite EMC shields,” *IEEE Trans. Magn.*, Vol. 49, No. 5, 1821–1824, May 2013.
8. Chung, Y. S., T. K. Sarkar, B. H. Jung, and M. Salazar-Palma, “An unconditionally stable scheme for the finite-difference time-domain method,” *IEEE Trans. Microw. Theory Tech.*, Vol. 51, No. 3, 697–704, Mar. 2003.
9. Chen, W.-J., W. Shao, and B.-Z. Wang, “ADE-Laguerre-FDTD method for wave propagation in general dispersive materials,” *IEEE Microw. Wireless Compon. Lett.*, Vol. 23, No. 5, 228–230, May 2013.
10. Chen, Z., Y. T. Duan, Y. R. Zhang, and Y. Yi, “A new efficient algorithm for the unconditionally stable 2-D WLP-FDTD method,” *IEEE Trans. Antennas Propag.*, Vol. 61, No. 7, 3712–3720, Jul. 2013.
11. Gandhi, O. P., B. Q. Gao, and J. Y. Chen, “A frequency-dependent finite-difference time-domain formulation for general dispersive media,” *IEEE Trans. Microw. Theory Tech.*, Vol. 55, No. 4, 703–708, Apr. 2007.
12. Ha, M. and M. Swaminathan, “A Laguerre-FDTD formulation for frequency-dependent dispersive materials,” *IEEE Microw. Wireless Compon. Lett.*, Vol. 21, No. 5, 225–227, May 2011.
13. Hanson, G. W., “Dyadic Greens functions and guided surface waves for a surface conductivity model of graphene,” *J. Appl. Phys.*, Vol. 103, No. 6, 064302, Mar. 2008.